

Effect of metoprolol on myocardial apoptosis and caspase-9 activation after coronary microembolization in rats

Qiang Su MD, Lang Li MD PhD, Yang-Chun Liu MD, You Zhou MD, Yong-Guang Lu MD, Wei-Ming Wen MD

Q Su, L Li, Y-C Liu, Y Zhou, Y-G Lu, W-M Wen. Effect of metoprolol on myocardial apoptosis and caspase-9 activation after coronary microembolization in rats. *Exp Clin Cardiol* 2013;18(2):161-165.

OBJECTIVE: To explore the effect of metoprolol on myocardial apoptosis and caspase-9 activation after coronary microembolization (CME) in rats.

METHODS: Forty rats were randomly divided into four groups (n=10 each): a sham operation (control) group, CME plus saline (CME) group, CME plus metoprolol (metoprolol) group and caspase-9 inhibitor Z-LEHD-FMK (ZLF) group. CME was induced by injecting 3000 polyethylene microspheres (42 µm diameter) into the left ventricle during a 10 s occlusion of the ascending aorta. Echocardiography, terminal deoxynucleotidyl transferase dUTP nick end labelling and Western blotting were used to evaluate cardiac function, apoptosis and activation of caspase-9/caspase-3, respectively, 6 h after CME.

Coronary microembolization (CME) is a serious complication that occurs in 10% to 40% of patients following percutaneous coronary intervention (PCI) to treat acute coronary syndromes. It occurs when atherosclerotic plaques rupture, and the thrombotic debris can directly induce 'no reflow' or 'slow flow' occurrences (1,2). CME is a progressive contractile dysfunction that develops in the presence of unchanged regional myocardial blood flow (3,4). Clinical outcomes in patients with CME are not improved by using coronary thrombolysis agents, nitroglycerin and platelet GPIIb/IIIa receptor antagonists, or direct thrombectomy (5,6) Therefore, appropriate therapy for CME remains an issue, and the underlying molecular mechanisms of CME pathophysiology remain to be elucidated.

CME is attracting increasing attention. Clinical studies have shown that intracoronary β-adrenergic blocker administration before PCI reduces CME-associated complications (7), and treatment with metoprolol before PCI significantly protects the ischemic myocardium from myocardial damage (8). Studies verified that intracoronary use of metoprolol can also reduce the occurrence of the 'no reflow' or 'slow flow' phenomenon and improve short- and long-term patient prognosis (9). Clinical findings showed that metoprolol exerted anti-inflammatory and antiapoptotic effects to improve cardiac function in patients with ischemic cardiomyopathy (8,10). In addition, we previously identified a significant improvement in left ventricular function in a rat model of CME following metoprolol treatment. The protection conferred by metoprolol against progressive contractile dysfunction following CME may be due to its anti-inflammatory potential (11). It is known that myocardial apoptosis occurs following CME (12), and metoprolol can inhibit the development of myocardial apoptosis. However, the potential role of metoprolol in the treatment of CME is not fully understood. Therefore, we sought to determine the effect of metoprolol pretreatment on myocardial apoptosis and caspase-9 activation (a key apoptotic protein in the mitochondrial apoptosis pathway) using a rodent model of CME. We tested the hypothesis that metoprolol pretreatment can ameliorate myocardial

RESULTS: The echocardiographic parameters of left ventricular function were significantly decreased in the CME group compared with the control group (P<0.05); however, the metoprolol group and ZLF group showed significantly improved cardiac function compared with CME alone (P<0.05). Compared with the control group, the myocardial apoptosis rate and the levels of activated caspase-9 and -3 increased significantly in the CME group (P<0.05). Again, these effects were ameliorated by metoprolol and ZLF (P<0.05).

CONCLUSIONS: The present study demonstrates that metoprolol and ZLF can protect the rat myocardium during CME by inhibiting apoptosis and improving cardiac function, likely by inhibiting apoptosis/mitochondrial apoptotic pathway. These results suggest that antiapoptotic therapies may be useful in treating CME.

Key Words: Apoptosis; Caspase-3; Caspase-9; Coronary microembolization; Metoprolol

dysfunction and suppress post-CME myocardial apoptosis by blocking mitochondria-mediated apoptosis.

METHODS

Animals and reagents

Male Sprague Dawley rats (200 g to 250 g) were supplied by the Animal Center of Guangxi Medical University (Nanning, China). All procedures were performed in accordance with institutional guidelines for animal care and the *Guide for Care and Use of Laboratory Animals* published by the US National Institutes of Health (NIH publication no. 85-23, revised 1996). Microembolization balls (lyophilized powder) were purchased from Dynal Corporation (Oslo, Norway). The diameter of the balls was 42 µm, there were 2×10⁷ balls in each gram of powder and the final density was 3×10⁴ balls/mL. Metoprolol was obtained from AstraZeneca Laboratories (Sweden). The caspase-9 inhibitor Z-LEHD-FMK (ZLF) and rabbit anti-rat caspase-9 were obtained from BioVision (USA). The rabbit anti-rat caspase-3 antibody was purchased from Cell Signaling Technology (USA). The terminal deoxynucleotidyl transferase dUTP nick end labelling (TUNEL) assay kit was purchased from Roche (USA).

Modelling and grouping

Rats were randomized into sham operation (control group), CME plus saline (CME group), CME plus metoprolol (metoprolol group) and caspase-9 inhibitor ZLF (ZLF group), with 10 rats in each group. The CME model was performed as described previously (13,14). Briefly, rats were anesthetized with 10% chloral hydrate (3 mL/kg intraperitoneally), and the trachea was intubated to maintain ventilation with a respirator. The chest was opened and the ascending aorta was isolated. Subsequently, 3000 microspheres suspended in 0.1 mL 0.9% saline were rapidly injected into the left ventricle during a 10 s occlusion of the ascending aorta. The occlusion device was removed following injection, and the chest was closed with sutures after heart and breathing rates returned to normal. Rats in the sham-operated control

Department of Cardiology, The First Affiliated Hospital of Guangxi Medical University, Nanning, China

Correspondence: Dr Lang Li, Department of Cardiology, The First Affiliated Hospital, Guangxi Medical University, Nanning 530021, China.

Telephone 86-0771-5331171, fax 86-0771-5359801, e-mail drllilang@163.com

TABLE 1
Cardiac function after coronary microembolization (CME)

Group	Number	LVEF, %	FS, %	CO, L/min	LVEDd, mm
Control	10	82.67±3.50	42.97±3.44	0.164±0.009	5.11±0.33
CME	10	72.88±3.27*	37.59±2.49*	0.102±0.007*	6.20±0.16*
Metoprolol	10	79.97±4.26†	41.64±2.08†	0.157±0.014†	5.34±0.29†
ZLF	10	76.34±4.41*†	39.35±2.24*†	0.136±0.018*†	5.67±0.33*†

* $P < 0.05$ compared with the control group; † $P < 0.05$ compared with the CME group. CO Cardiac output; FS Fractional shortening; LVEDd Left ventricular end-diastolic diameter; LVEF Left ventricular ejection fraction; ZLF Z-LEHD-FMK

group were administered saline without microspheres. Rats in the metoprolol group received three intravenous bolus injections of metoprolol (2.5 mg/kg) at approximately 5 min intervals beginning 30 min before CME induction, and the CME group received equivalent saline injections.

Echocardiography

The rats were lightly anesthetized with an intraperitoneal injection of sodium pentobarbital (30 mg/kg to 40 mg/kg) and the left ventricle was examined using echocardiography. Briefly, a 12 MHz transducer was placed on the left anterior chest wall to obtain left ventricle ejection fraction (LVEF), left ventricle end-diastolic dimension (LVEDd), fractional shortening (FS) and cardiac output (CO). All echocardiographic measurements were performed by an experienced physician using a Philips Sonos 7500 system (Philips, USA). Cardiac function evaluation was performed three times, and the mean of each index was used.

Tissue sampling

After echocardiography, the hearts were arrested in diastole by injecting 2 mL 10% KCl into the tail vein. The heart was immediately removed, the atrial appendage and atrium cordis were removed, and the heart ventricle was separated into apex and base segments from the midpoint of the left ventricle long axis along the direction parallel to the atrioventricular groove. The apex was rapidly frozen in liquid nitrogen and stored at -80°C until preparation for Western blot analysis. The base was fixed in 4% paraformaldehyde for 12 h, embedded in paraffin and serially sectioned (4 μm thick; ≥ 12 section per animal). Three sections containing the same number of microinfarct foci were selected for TUNEL staining to detect myocardial apoptosis, and hematoxylin and eosin staining and hematoxylin-basic fuchsin-picric acid (HBFP) staining were performed on triplicate slices to assess myocardial microinfarction area.

Measuring myocardial microinfarction area

HBFP staining is an important method for the early diagnosis of myocardial ischemia. It dyes ischemic cardiac muscle, normal myocardial cytoplasm and nuclei red, yellow and blue, respectively. A DMR-Q550 pathological image pattern analysis instrument (Leica, Germany) was used to analyze HBFP-stained slices. Briefly, five microscopic visual fields (original magnification $\times 100$) were randomly sampled from each slice for observation using QWin analysis software (Leica, Germany) and the planar area method was used to measure the infarction zone, which was expressed as an area per cent of bulk analysis slice and averaged (12). The relative ischemic area was calculated according to the following formula: ischemic area/total area $\times 100\%$.

TUNEL assay

TUNEL staining was performed according to the manufacturer's instructions. The apoptotic nuclei were stained a yellow-brown colour (TUNEL-positive), and a total of 40 nonoverlapping zones ($\times 400$) belonging to the microinfarction zone, the marginal zone and the zone far from infarction from each slice were randomly observed (15). The

number of apoptotic cardiomyocytes and overall cell number were determined, and the myocardial apoptotic rate was calculated as the number of apoptotic cells/total number of cells $\times 100\%$.

Western blot assay

To detect activated caspase-9 and -3 in myocardial tissues, antibodies recognizing shear-activated caspase-9 and -3 were used in Western blot assays. Total protein was extracted using lysis buffer, and the Lowry method was used to measure protein concentration. We performed sodium dodecyl sulfate-polyacrylamide gel electrophoresis by loading 50 μg of each sample on 10% polyacrylamide gels, then transferring the separated proteins to a polyvinylidene fluoride membrane using 100 mA current for 2 h. The membrane was then incubated in blocking solution at room temperature for 1 h, rinsed with Tris-buffered saline with Tween-20, incubated with primary antibody (caspase-9 or cleaved caspase-3, 1:1000) overnight at 4°C , rinsed again with Tris-buffered saline with Tween-20, and incubated with horseradish peroxidase-conjugated secondary antibodies (1:2000) at room temperature for 1 h. Horseradish peroxidase-labelled anti-glyceraldehyde-3-phosphate dehydrogenase (GAPDH) (1:1000) served as an internal loading control. A Bio-Rad Gel Doc 2000 imaging system and software (Hercules, USA) were used to calculate the integrated absorbance (IA) of the identified bands according to the following formula: IA = area \times average density. After normalizing bands to GAPDH levels, the ratios of caspase-3 and -9 IA to GAPDH IA were used to represent the relative levels of activated caspase-3 and -9.

Statistical analysis

Measurement data are expressed as mean \pm SD. Comparisons were performed using unpaired Student's *t* tests (two groups) or ANOVAs (three or more groups) followed by Tukey's post hoc tests. For linear correlation analysis, the Pearson correlation coefficient *R* was computed using SPSS software (IBM Corporation, USA). $P < 0.05$ was considered to be statistically significant.

RESULTS

Animal groups

No statistically significant differences ($P > 0.05$) were observed in body weight or heart rate among the four groups (data not shown).

Changes of cardiac function index

Cardiac ultrasonography (Table 1) showed that 6 h after surgery, the CME group exhibited significantly decreased cardiac function compared with the control group, which manifested as systolic dysfunction and left ventricle dilation with significant decreases in LVEF, FS and CO; however, LVEDd was significantly increased ($P < 0.05$). Metoprolol pretreatment improved all indices of cardiac function in CME-treated animals. Specifically, LVEF, FS and CO were significantly increased and LVEDd was significantly decreased ($P < 0.05$) compared with the CME group. ZLF improved CME-induced cardiac dysfunction; the ZLF group had significantly higher LVEF, FS and CO and lower LVEDd compared with the CME group ($P < 0.05$).

Effects of metoprolol and ZLF on myocardial infarction size

Microspheres were injected directly into the coronary arteries, and effective CME was evident by histology (Figure 1). However, there was no significant difference ($P > 0.05$) in myocardial infarct size in the metoprolol and ZLF groups compared with the CME group (Figure 2). Infarct areas in the CME, metoprolol and ZLF groups were $8.32 \pm 3.27\%$, $7.98 \pm 2.72\%$, and $7.74 \pm 2.58\%$, respectively.

Effects of metoprolol and ZLF treatment on myocardial apoptosis

Apoptosis was assessed using TUNEL staining. Compared with the control group, there were many TUNEL-positive (brown) cells in the CME-treated hearts ($P < 0.05$). Metoprolol and ZLF treatment significantly decreased ($P < 0.05$) the relative proportion of apoptotic cells

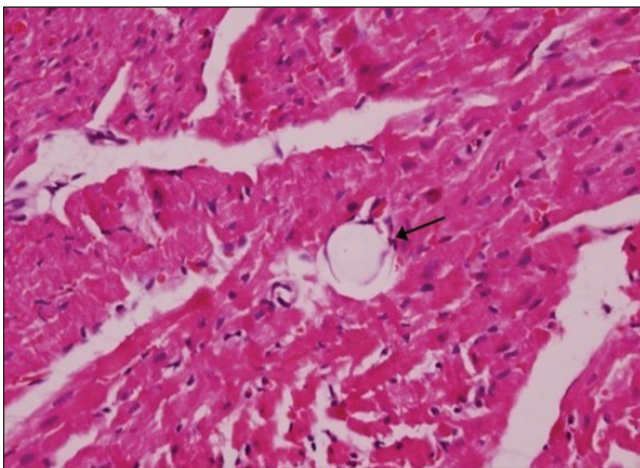


Figure 1 Histopathology of postcoronary microembolization myocardial microinfarcts (original magnification $\times 400$). Hematoxylin and eosin staining of tissue samples from the coronary microembolization group reveals myocardial microinfarcts with a low level of inflammatory cell infiltration. However, a portion of the cardiomyocyte nuclei is not visible. The arrow indicates the presence of a $42 \mu\text{m}$ microsphere after the experimental protocol

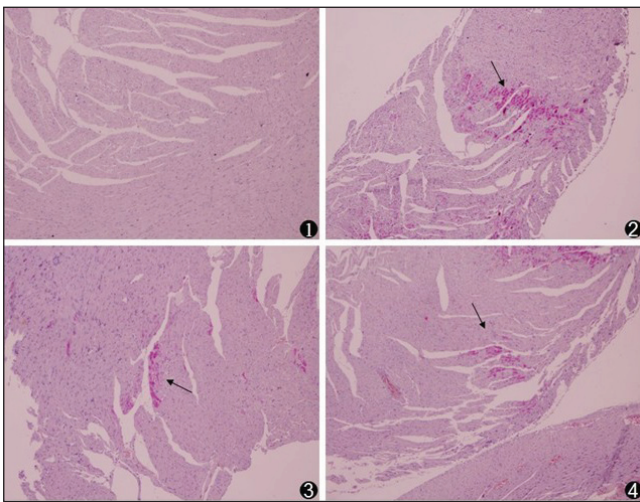


Figure 2 Histopathology of myocardial microinfarcts (original magnification $\times 100$). Hematoxylin-basic fuchsin-picric acid staining of tissue samples revealed no infarct in the sham-operated (control, 1) animals. Microinfarcts (arrows) in the tissue samples from coronary microembolization (2), metoprolol (3) and Z-LEHD-FMK (4) groups. Normal myocardial cytoplasm is stained yellow, the nuclei are stained blue and the ischemic myocardium is stained red

following CME. The myocardial apoptotic percentages in the control, CME, metoprolol and ZLF groups were $0.20 \pm 0.15\%$, $3.17 \pm 1.26\%$, $1.32 \pm 0.28\%$ and $1.14 \pm 0.31\%$, respectively (Figures 3 and 4).

Effect of metoprolol on caspase-9 and -3 expression

Because metoprolol and ZLF treatments decreased apoptosis in CME rats, Western blot analysis of mitochondrial apoptotic pathway proteins, including activated caspase-9 and -3 (Figures 5 and 6), was performed. Compared with the control group, the CME group showed significantly enhanced expression of activated caspase-9 and -3 ($P < 0.05$). Compared with the CME group, the metoprolol group exhibited significantly decreased levels of activated caspase-9 and -3 ($P < 0.05$). ZLF also inhibited activated caspase-9 expression and decreased caspase-3 levels ($P < 0.05$).

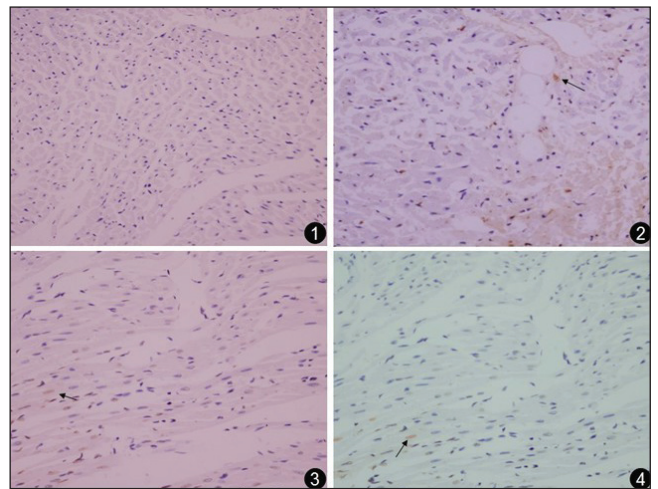


Figure 3 Photomicrographs showing the effect of metoprolol on apoptosis following coronary microembolization (original magnification $\times 400$). The terminal deoxynucleotidyl transferase dUTP nick end labelling assay reveals myocardial apoptosis in control (1), coronary microembolization (2), metoprolol (3) and Z-LEHD-FMK (4) groups. Normal cell nuclei are stained pale blue, while the apoptotic cardiomyocyte nuclei (arrows) are stained brown

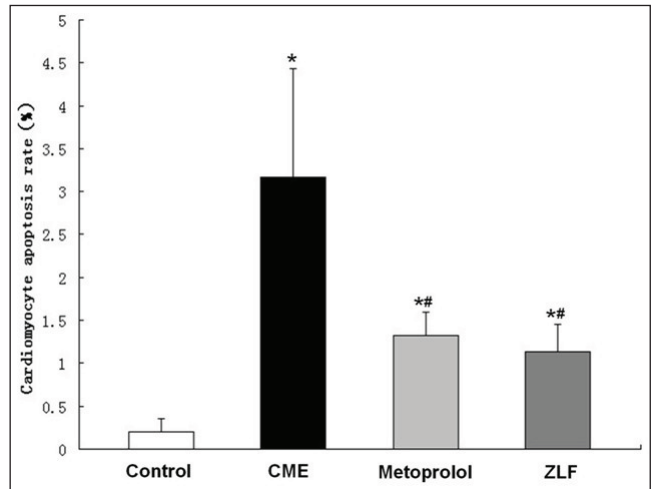


Figure 4 Graph showing the effect of metoprolol on apoptosis following coronary microembolization (CME). Cells that stained positive in the terminal deoxynucleotidyl transferase dUTP nick end labelling assay after CME were detected primarily in myocardial microinfarction foci and the peripheral zones. In control animals, myocardial apoptosis was occasionally found in the subendocardium and papillary muscles. Data ($n = 10$ per group) are expressed as mean \pm SD. * $P < 0.05$ compared with the control group; # $P < 0.05$ compared with the CME group. ZLF Z-LEHD-FMK

Linear correlation analysis

Linear correlation analysis indicated that the level of activated caspase-9 was positively correlated with activated caspase-3 ($r = 0.788$; $P = 0.012$), and with relative apoptotic cell proportion ($r = 0.932$; $P = 0.006$). Additionally, activated caspase-3 was positively correlated with relative apoptotic cell proportion ($r = 0.856$; $P = 0.029$).

DISCUSSION

CME is a frequent and serious event in patients with ischemic heart disease (2). It may occur spontaneously in patients with acute coronary syndromes or artificially during thrombolytic therapy and coronary interventions, resulting in typical consequences such as malignant arrhythmias and contractile dysfunction. Atherothrombotic debris released into coronary microcirculation is

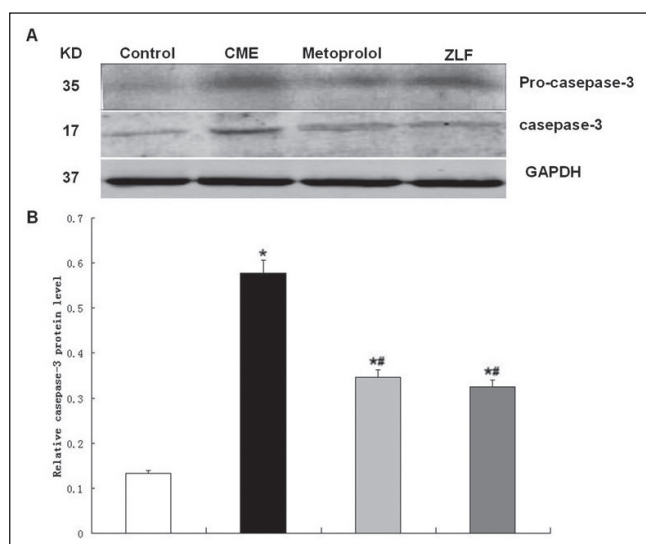


Figure 5 Effect of metoprolol on caspase-3 expression following coronary microembolization (CME). **A** The relative protein levels of procaspase-3 and activated caspase-3 were determined using Western blots (normalized to glyceraldehyde-3-phosphate dehydrogenase [GAPDH]). Lanes 1, 2, 3 and 4 in the representative gel show caspase-3 expression in control, CME (after 6 h), metoprolol and Z-LEHD-FMK (ZLF) groups, respectively. **B** The graphed data (n=10 per group) represent mean \pm SD. * $P < 0.05$ compared with the control group; # $P < 0.05$ compared with the CME group

believed to cause distal microembolization. CME is an independent predictor of long-term poor prognosis in patients with acute myocardial infarction that causes transient 'no blood flow' or 'slow flow' (16,17). Previous studies have demonstrated that during the acute phase after CME, the local myocardium exhibited microinfarction foci, myocardial cells underwent necrosis and apoptosis, and cardiac function progressively declined (12). Interestingly, intravenous β -blocker treatment before coronary artery occlusion markedly reduced myocardial injury (18). Clinical studies have also indicated that intravenous metoprolol can significantly protect the heart during ischemia-reperfusion (8).

Our preliminary experiment revealed that caspase-9 was activated after CME and that levels peaked 6 h after CME, so we adopted that time point in the present study. Notably, we found multiple microinfarction foci in the myocardium, apoptotic and necrotic myocardial cells, and decreased cardiac function.

Caspases are a family of aspartic acid-specific proteases that are the major effectors of apoptosis. In healthy cells, they exist as inactive zymogens that are activated by a signalling cascade at the onset of apoptosis (19), which is mediated by caspase-3. Undergoing metoprolol intracoronary injection before surgery could significantly reduce myocardial apoptosis and improve decreased systolic dysfunction caused by CME. Our results suggest that these effects would be achieved by inhibiting the expression of activated caspase-3 and -9. Cardiac echocardiography revealed systolic dysfunction and left ventricular dilation manifested by a decrease in LVEF, FS and CO, as well as an increase in LVEDd. Because myocardial cells are nondifferentiating, inhibition of myocardial apoptosis may be one of the most important mechanisms by which metoprolol therapy improves CME prognosis.

Apoptosis can be induced by activation of cell surface death receptors and mitochondrial or endoplasmic reticulum pathways. The active form of caspase-9 is an initiator caspase in the mitochondrial apoptosis cascade (20). Cleaved caspase-9 goes on to cleave procaspase-3 and procaspase-7, which cleave several cellular targets, including poly-ADP ribose polymerase, ultimately inducing apoptosis (21). There are numerous reports that caspase-9 (22,23) and caspase-3

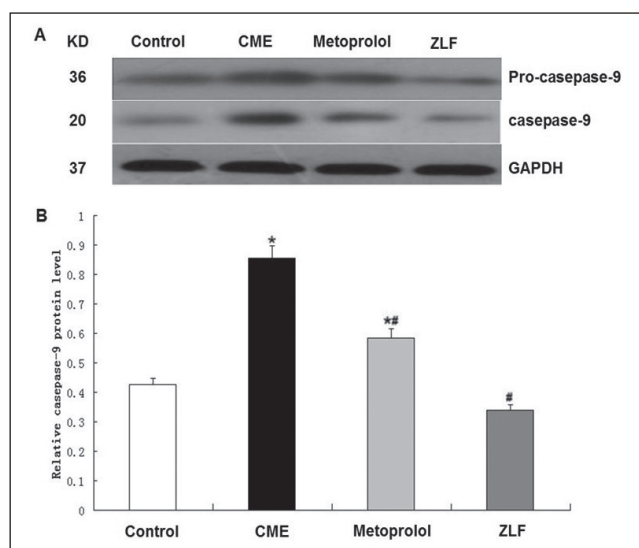


Figure 6 Effect of metoprolol on caspase-9 expression following coronary microembolization (CME). **A** The relative protein levels of procaspase-9 and activated caspase-9 were determined using Western blots (normalized to glyceraldehyde-3-phosphate dehydrogenase [GAPDH]). Lanes 1, 2, 3 and 4 in the representative gel show caspase-9 expression in the control, CME (after 6 h), metoprolol and Z-LEHD-FMK (ZLF) groups, respectively. **B** Bars (n=10) represent mean \pm SD. * $P < 0.05$ compared with the control group; # $P < 0.05$ compared with the CME group

(24,25) participate in myocardial infarction progression. One study (21) demonstrated that myocardial ischemia-induced apoptosis can be effectively prevented by inhibiting the assembly of the Apaf-1/caspase-9 apoptosome. Therefore, caspase-9 is an important promoter of the mitochondrial apoptosis pathway.

Here, we showed that metoprolol pretreatment significantly decreased activated caspase-9 protein expression in a rodent model of CME. This inhibitory effect was the same as that achieved using ZLF (specific inhibitor of caspase-9), indicating that metoprolol-mediated inhibition of myocardial apoptosis involves the mitochondria-mediated apoptosis pathway.

Nevertheless, our study also has some limitations that need to be addressed. First, there is a definite need for a more suitable animal model that accurately mimics the clinical scenario of CME. Polymer microspheres do not have the biochemical characteristics of natural microemboli, including platelets, endothelial cells and plaque debris with cholesterol crystals. Second, natural emboli exhibit a wide range of sizes and shapes. The microspheres used to induce CME in this study may not fully reflect the nature of clinical CME.

In summary, we have shown that mitochondrial apoptosis was increased in CME-lesioned rat tissues, as evidenced by TUNEL staining and caspase-9/caspase-3 activation. Treatment with metoprolol or the caspase-9 inhibitor ZLF significantly attenuated CME-induced myocardial injury and improved cardiac function. Thus, our results indicate that metoprolol and ZLF protect the myocardium by inhibiting apoptosis and may shed light on the potential importance of the mitochondrial apoptotic pathway in CME therapies.

ACKNOWLEDGEMENT: This study was supported by a grant from National Natural Science Foundation of China (Grant No. 30760262/C030313).

DISCLOSURES: This article has not been published elsewhere in whole or in part. All authors have read and approved the content and agreed to submit for consideration for publication in the *Journal*. There are no ethical or legal conflicts involved in the article.

REFERENCES

1. Heusch G, Kleinbongard P, Bose D, et al. Coronary microembolization: From bedside to bench and back to bedside. *Circulation* 2009;120:1822-36.
2. Morishima I, Sone T, Okumura K, et al. Angiographic no-reflow phenomenon as a predictor of adverse long-term outcome in patients treated with percutaneous transluminal coronary angioplasty for first acute myocardial infarction. *J Am Coll Cardiol* 2000;36:1202-9.
3. Dorge H, Neumann T, Behrends M, et al. Perfusion-contraction mismatch with coronary microvascular obstruction: Role of inflammation. *Am J Physiol Heart Circ Physiol* 2000;279:H2587-92.
4. Carlsson M, Martin AJ, Ursell PC, Saloner D, Saeed M. Magnetic resonance imaging quantification of left ventricular dysfunction following coronary microembolization. *Magn Reson Med* 2009;61:595-602.
5. Waksman R, Douglas JS, Jr, Scott NA, Ghazzal ZM, Yee-Peterson J, King SB 3rd. Distal embolization is common after directional atherectomy in coronary arteries and saphenous vein grafts. *Am Heart J* 1995;129:430-5.
6. Grube E, Schofer JJ, Webb J, et al. Evaluation of a balloon occlusion and aspiration system for protection from distal embolization during stenting in saphenous vein grafts. *Am J Cardiol* 2002;89:941-5.
7. Prabhu SD, Chandrasekar B, Murray DR, Freeman GL. Beta-adrenergic blockade in developing heart failure: Effects on myocardial inflammatory cytokines, nitric oxide, and remodeling. *Circulation* 2000;101:2103-9.
8. Wang FW, Osman A, Otero J, et al. Distal myocardial protection during percutaneous coronary intervention with an intracoronary beta-blocker. *Circulation* 2003;107:2914-9.
9. Uretsky BF, Birnbaum Y, Osman A, et al. Distal myocardial protection with intracoronary beta blocker when added to a Gp IIb/IIIa platelet receptor blocker during percutaneous coronary intervention improves clinical outcome. *Catheter Cardiovasc Interv* 2008;72:488-97.
10. Ahmet I, Krawczyk M, Heller P, Moon C, Lakatta EG, Talan MI. Beneficial effects of chronic pharmacological manipulation of beta-adrenoreceptor subtype signaling in rodent dilated ischemic cardiomyopathy. *Circulation* 2004;110:1083-90.
11. Lu Y, Li L, Zhao X, Huang W, Wen W. Beta blocker metoprolol protects against contractile dysfunction in rats after coronary microembolization by regulating expression of myocardial inflammatory cytokines. *Life Sci* 2011;88:1009-15.
12. Thielmann M, Dorge H, Martin C, et al. Myocardial dysfunction with coronary microembolization: Signal transduction through a sequence of nitric oxide, tumor necrosis factor-alpha, and sphingosine. *Circ Res* 2002;90:807-13.
13. Li L, Li DH, Qu N, Wen WM, Huang WQ. The role of ERK1/2 signaling pathway in coronary microembolization-induced rat myocardial inflammation and injury. *Cardiology* 2010;117:207-15.
14. Kalenikova EI, Gorodetskaya EA, Zacharova NV, Shechter AB, Medvedev OS. Perindopril effects on angiotensin I elimination in lung after experimental myocardial injury induced by intracoronary microembolization in rats. *J Cardiovasc Pharmacol* 1998;32:608-15.
15. Zhang QY, Ge JB, Chen JZ, et al. Mast cell contributes to cardiomyocyte apoptosis after coronary microembolization. *J Histochem Cytochem* 2006;54:515-23.
16. Kawano H, Hayashida T, Ohtani H, et al. Histopathological findings of the no-reflow phenomenon following coronary intervention for acute coronary syndrome. *Int Heart J* 2005;46:327-32.
17. Jaffe R, Charron T, Puley G, Dick A, Strauss BH. Microvascular obstruction and the no-reflow phenomenon after percutaneous coronary intervention. *Circulation* 2008;117:3152-6.
18. Miura M, Thomas R, Ganz W, et al. The effect of delay in propranolol administration on reduction of myocardial infarct size after experimental coronary artery occlusion in dogs. *Circulation* 1979;59:1148-57.
19. Holleyman CR, Larson DF. Apoptosis in the ischemic reperfused myocardium. *Perfusion* 2001;16:491-502.
20. Kuida K. Caspase-9. *Int J Biochem Cell Biol* 2000;32:121-4.
21. Puyal J, Vaslin A, Mottier V, Clarke PG. Postischemic treatment of neonatal cerebral ischemia should target autophagy. *Ann Neurol* 2009;66:378-89.
22. Takatani T, Takahashi K, Uozumi Y, et al. Taurine inhibits apoptosis by preventing formation of the Apaf-1/caspase-9 apoptosome. *Am J Physiol Cell Physiol* 2004;287:C949-53.
23. Mocanu MM, Baxter GF, Yellon DM. Caspase inhibition and limitation of myocardial infarct size: Protection against lethal reperfusion injury. *Br J Pharmacol* 2000;130:197-200.
24. Yue TL, Wang C, Romanic AM, et al. Staurosporine-induced apoptosis in cardiomyocytes: A potential role of caspase-3. *J Mol Cell Cardiol* 1998;30:495-507.
25. Balsam LB, Kofidis T, Robbins RC. Caspase-3 inhibition preserves myocardial geometry and long-term function after infarction. *J Surg Res* 2005;124:194-200.